Performance of RIS-aided Media-Based Modulation with Imperfect CSI and Phase Tuning Errors

Shankul Saini and A. Chockalingam
Department of ECE, Indian Institute of Science, Bangalore 560012

***Abstract*—Reconfigurable intelligent surface (RIS) technology uses electronically tunable surfaces in the far field of the transmit antenna for the purpose of beamforming towards receiver of interest. Media-based modulation (MBM) uses such surfaces in the near field of the transmit antenna for the purpose of modulation. RIS-aided MBM offers improved communication performance at low radio-frequency (RF) hardware complexity, combining the good attributes of both RIS and MBM. In this paper, we analyze the performance of RIS-aided MBM in the presence of imperfect channel state information (CSI) at the receiver and phase tuning errors at the RIS. We derive expressions for pairwise error probability and bit error probability for RIS-aided MBM with imperfect CSI and phase tuning errors. Bit error rate performance results obtained through analysis and simulations are presented. Results show improved bit error performance for increased number of RIS elements.**

***Index Terms*—Reconfigurable intelligent surface, media-based modulation, RIS-aided MBM, imperfect CSI, phase tuning error.**

I. Introduction

Reconfigurable intelligent surface (RIS) technology [1]- [3] and media-based modulation (MBM) [4]- [8] are promising physical layer techniques in wireless communication. RIS and MBM make use of intelligent surfaces differently for different purposes. First, RIS uses intelligent surfaces for the purpose of beamforming, whereas MBM uses such surfaces for the purpose of modulation. Second, the intelligent surfaces in RIS are placed in the far field of the transmit antenna, whereas in MBM they are placed in the near field of the transmit antenna. Third, the reflecting elements in RIS are phase tuned in such a way that the incident wave from the transmitter is steered towards the direction of the receiver, and, in doing so, the signal-to-noise ratio in the direction of the receiver is maximized. In MBM, the refelecting elements are called RF mirrors. The RF mirrors are controlled by information bits. The RF mirrors can be viewed as digitally controlled near-field scatterers. When a mirror is excited with a digital 1, it becomes 'RF opaque', i.e., it blocks the incident RF energy from the transmit antenna. When excited with a digital 0, it becomes 'RF transparent', i.e., it allows the incident RF energy from the transmit antenna to pass through. Such digitally controlled perturbations in the near-field propagation characteristics results in different fade coefficients at the far-field receiver for different bit patterns that excite the mirrors. These fade coefficients act as the modulation symbols, and hence the name media (i.e., channel) based modulation.

This work was supported by the J. C. Bose National Fellowship, Department of Science and Technology, Government of India.

Both RIS and MBM are power efficient and RF hardware efficient techniques. For example, the reflecting elements in RIS and RF mirrors in MBM can be realized using simple diodes, varactors, switched capacitors, etc. Also, MBM is a spectrally efficient modulation, where the achieved rate increases linearly with the number of RF mirrors used. Therefore, the idea of using intelligent surfaces both at the near field (for MBM) and far field (for beamforming) is an attractive proposition that can bring in spectral efficiency and power efficiency benefits at low RF hardware complexity/cost [9]. Such RIS-aided MBM schemes deserve detailed investigations, which forms the motivation and focus in this paper.

In this paper, we consider an MBM system aided by RIS, develop its system model, and analyze its bit error performance. In the study, we consider two important aspects of practical importance, namely, imperfect channel state information (CSI) and phase tuning errors at the RIS. In MBM, the set of channel fade coefficients corresponding to all possible information bit patterns that activate the RF mirrors form the modulation alphabet. The performance of MBM (without RIS aid) in the presence of imperfect CSI has been analyzed in [10], [11]. In RIS-aided MBM, the modulation alphabet is due to the fades on the transmitter-to-RIS link and RIS-to-receiver link, and the phase rotations caused by the RIS elements. It is of interest to analyze the effect of errors in the estimated modulation alphabet (i.e., imperfect CSI) on the performance of RIS-aided MBM. Likewise, in RIS, there can be errors in the phases that tune RIS elements (e.g., due to phase quantization and other imperfections), which affect performance. BER performance of RIS with phase errors have been analyzed in the literature, e.g., [12]. However, performance analysis of RIS-aided MBM in the presence of imperfect CSI and RIS phase tuning errors has not been reported so far. In this paper, we present such an analysis. Specifically, we derive expressions for the pairwise error probability (PEP) and bit error probability for RIS-aided MBM with imperfect CSI and phase tuning errors. We present bit error rate performance results obtained through analysis and simulations. Analytical and simulation results show improved bit error performance for increasing number of RIS elements.

The rest of the paper is organized as follows. The considered RIS-aided MBM system model is presented in Sec. II. The performance analysis is carried out in Sec. III. Performance results and discussions are presented in Sec. IV. Conclusions are presented in Sec. V.

Notations: A matrix is represented by an uppercase boldface

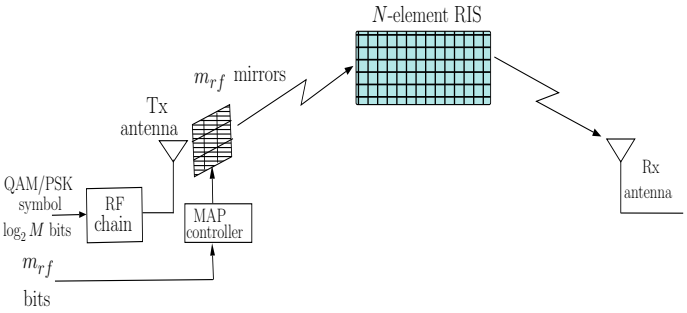

Fig. 1: RIS-aided MBM system.

letter, a vector by a lowercase boldface letter, and a diagonal matrix by $\text{diag}\{x_1, \cdots, x_n\}$. The determinant of a matrix is denoted by $\det(\cdot)$. An identity matrix of size $K \times K$ is denoted by $\mathbf{I}_K$. $(.)^*$, $(\cdot)^T$, $(\cdot)^H$, $\mathbb{E}[\cdot]$ and $\Re(.)$ represent complex conjugate, transposition, Hermitian, expectation and real operators, respectively. A complex Gaussian distribution and a Normal distribution with mean μ and variance σ^2 is denoted by $\mathcal{CN}(\mu, \sigma^2)$ and $\mathcal{N}(\mu, \sigma^2)$ respectively. $|.|$, $\|.\|_2$ denote the magnitude of a complex number, 2-norm of a vector, respectively and $\mathbb{C}$ represents the set of complex-valued numbers.

II. RIS-aided MBM system model

This section presents the system model of the considered RIS-aided MBM system with imperfect CSI and RIS phase tuning errors.

A. RIS-aided MBM system

The RIS-aided MBM system consists of an MBM transmitter, an MBM receiver, and an RIS to aid the transmission from the transmitter to the receiver as shown in Fig. 1. The transmitter consists of one transmit antenna and m_{rf} RF mirrors placed in its near-field. The RIS consists N phase tunable elements. In a given channel use, an information symbol from an M-ary modulation alphabet $\mathbb{A}$ (e.g., QAM/PSK) is transmitted by the transmit antenna and m_{rf} information bits excite the m_{rf} RF mirrors. Therefore, the transmitter conveys a total of $m_{rf}+\log_2 M$ information bits in one channel use. The pattern of ones and zeros in the m_{rf} bits that excite mirrors is called the mirror activation pattern (MAP). There are $2^{m_{rf}}$ possible MAPs. Excitation of the mirrors with different MAPs results in $2^{m_{rf}}$ different fade coefficients at the receiver. This set of $2^{m_{rf}}$ fade coefficients form the channel modulation alphabet. The transmit signal set $\mathbb{S}$ consists of $2^{m_{rf}}$ transmit signal vectors, which are 1-sparse vectors, given by

$$\mathbb{S} = \{\mathbf{s} : \ s_i \in \mathbb{A} \cup 0, \ \|\mathbf{s}\|_0 = 1\}, \tag{1}$$

where $\mathbf{s}$ is a $2^{m_{rf}} \times 1$ vector, s_i is the ith element of $\mathbf{s}$, and $\|\cdot\|_0$ denotes the l_0-norm of a vector.

Let $\mathbf{h}^k = [h_1^k \ h_2^k \cdots h_{2^{m_{rf}}}^k]$ denote the $1 \times 2^{m_{rf}}$ vector of channel coefficients between the transmitter and kth RIS element, $k = 1, 2, \cdots, N$, where $h_j^k \sim \mathcal{CN}(0, 1)$ is the channel fade coefficient corresponding to the jth MAP, $j = 1, 2, \cdots, 2^{m_{rf}}$. Let $\mathbf{\Phi} \triangleq \text{diag}\{e^{j\phi_1}, \cdots, e^{j\phi_N}\}$ denote the phase matrix at the RIS, where ϕ_i is tuning phase of the ith element in the RIS. Let $\mathbf{g} \triangleq [g^1, g^2, \cdots, g^N] \in \mathbb{C}^{1\times N}$ denote the vector of channel coefficients between the RIS and the receiver, where $g^i \sim \mathcal{CN}(0, 1)$ is the channel fade coefficient between the ith RIS element, $i = 1, 2, \cdots, N$, and the receive antenna. The received symbol y at the receiver is given by

$$y = \left[\sum_{i=1}^{N} g^i e^{j\phi_i} \mathbf{h}^i\right] \mathbf{x} + n, \tag{2}$$

where n denotes the additive noise at the receiver. Equation (2) can be written as

$$\begin{aligned} y &= \mathbf{g}\Phi\mathbf{H}\mathbf{x} + n \\ &= \mathbf{p}\mathbf{x} + n, \end{aligned} \tag{3}$$

where $\mathbf{H} \triangleq [(\mathbf{h}^1)^T \ (\mathbf{h}^2)^T \cdots \ (\mathbf{h}^N)^T]^T \in \mathbb{C}^{N\times 2^{m_{rf}}}$, and $\mathbf{p} \triangleq \mathbf{g}\Phi\mathbf{H}$ is the end-to-end composite channel vector of length $1 \times 2^{m_{rf}}$. The maximum likelihood (ML) detection is given by

$$\hat{\mathbf{x}} = \underset{\mathbf{x}\in\mathbb{S}}{\text{argmin}} \, |y - \mathbf{p}\mathbf{x}|^2. \tag{4}$$

The detected vector $\hat{\mathbf{x}}$ is demapped back to M-ary symbol and MAP bits.

B. Channel estimation error

The knowledge of the composite channel vector $\mathbf{p}$ is required at the receiver to detect the transmit vector $\mathbf{x}$. The estimation of the composite channel coefficients is done using pilot-based estimation techniques. The estimate $\hat{p}_i$ of the ith path's composite channel coefficient p_i can be written as

$$\hat{p}_i = p_i + e_i, \quad i = 1, 2, \cdots, 2^{m_{rf}}, \tag{5}$$

where e_i denotes the error in the estimate of the ith path's composite channel coefficient, and e_is are assumed to be i.i.d, independent of p_is, and distributed as $\mathcal{CN}(0, \sigma_e^2)$, where σ_e^2 is the variance of the estimation error. Let $\hat{\mathbf{p}}$ and $\mathbf{e}$ denote the estimated channel vector and corresponding error vector, respectively. From (5), $\hat{\mathbf{p}}$ can be written as

$$\hat{\mathbf{p}} = \mathbf{p} + \mathbf{e}. \tag{6}$$

Here (6) models the imperfection in estimating the composite channel vector at the receiver in the RIS-aided MBM system. Note that the elements of $\hat{\mathbf{p}}$ are distributed as $\mathcal{CN}(0, 1 + \sigma_e^2)$, where σ_e^2 is the parameter that represents the channel estimation accuracy, and $\sigma_e^2 = 0$ corresponds to perfect CSI at receiver, i.e., $\hat{\mathbf{p}} = \mathbf{p}$.

C. Phase tuning error at the RIS

In RIS, the optimal phase shift at the ith reflecting element, given by $\phi_i = -(\angle h_k^i + \angle g^i)$, is desired to maximize the received signal power at the receiver. However, due to imperfections in implementation, there can be errors in the actual phase shifts compared to the true optimal phase shifts. To account for this, we assume that the phase shift at the ith reflecting element is given by $\phi_i' = \phi_i - \phi_i^e$, where ϕ_i^e is the error in the phase shift and it is assumed to follow uniform distribution, i.e., $\phi_i^e \sim \text{U}[-\frac{\pi}{L}, \frac{\pi}{L}]$, where a large value of L corresponds to a low phase tuning error.

III. Performance Analysis

In this section, we carry out the performance analysis of the RIS-aided MBM system described in the previous section.

A. BER analysis with imperfect CSI at receiver

Consider that the estimated composite channel vector $\hat{\mathbf{p}}$ is available at the receiver. The decision rule, in this case, is

$$\hat{\mathbf{x}} = \underset{\mathbf{x}\in\mathbb{S}}{\operatorname{argmin}} |y - \hat{\mathbf{p}}\mathbf{x}|^2. \tag{7}$$

The conditional pairwise error probability (PEP) of transmitted signal vector $\mathbf{x}_1$ being decoded as $\mathbf{x}_2$ can be written as

$$P(\mathbf{x}_1 \to \mathbf{x}_2 \mid \hat{\mathbf{p}}) = P(|y - \hat{\mathbf{p}}\mathbf{x}_1|^2 > |y - \hat{\mathbf{p}}\mathbf{x}_2|^2). \tag{8}$$

Using (3) and (6), (8) can be written as

$$\begin{aligned} &P(\mathbf{x}_1 \to \mathbf{x}_2 \mid \hat{\mathbf{p}}) \\ &= P\big(\,|(\hat{\mathbf{p}} - \mathbf{e})\mathbf{x}_1 + n - \hat{\mathbf{p}}\mathbf{x}_1|^2 > |(\hat{\mathbf{p}} - \mathbf{e})\mathbf{x}_1 + n - \hat{\mathbf{p}}\mathbf{x}_2|^2\,\big) \\ &= P\big(\,|n - \mathbf{e}\mathbf{x}_1|^2 > |\hat{\mathbf{p}}(\mathbf{x}_1 - \mathbf{x}_2) + n - \mathbf{e}\mathbf{x}_1|^2\,\big) \\ &= P\big(\Re\{(\hat{\mathbf{p}}(\mathbf{x}_1 - \mathbf{x}_2))^*(\mathbf{e}\mathbf{x}_1 - n)\} > \frac{1}{2}\,|\hat{\mathbf{p}}(\mathbf{x}_1 - \mathbf{x}_2)|^2\,\big). \end{aligned} \tag{9}$$

We have $n \sim \mathcal{CN}(0, \sigma^2)$ and $\mathbf{e} \sim \mathcal{CN}(0, \sigma_e^2)$. So, $\Re(\mathbf{e}\mathbf{x_1} - n) \sim \mathcal{N}(0, \frac{1}{2}(\sigma^2 + \|\mathbf{x}_1\|_2^2\,\sigma_e^2))$. Defining $\psi = \hat{\mathbf{p}}(\mathbf{x}_1 - \mathbf{x}_2)$, we can write $\Re(\psi^*(\mathbf{e}\mathbf{x}_1 - n)) \sim \mathcal{N}(0, \frac{1}{2}|\psi|^2(\sigma^2 + \|\mathbf{x}_1\|_2^2\,\sigma_e^2))$. Therefore,

$$\begin{aligned} P(\mathbf{x}_1 \to \mathbf{x}_2 \mid \hat{\mathbf{p}}) \;&=\; P\big(\Re(\psi^*(\mathbf{e}\mathbf{x}_1 - n)) > \frac{1}{2}|\psi|^2\big) \\ &= Q\left(\sqrt{\frac{|\psi|^2}{2(\sigma^2 + \|\mathbf{x}_1\|_2^2\,\sigma_e^2)}}\right), \end{aligned} \tag{10}$$

where σ^2 is the noise power. Now, using $Q(x) = \frac{1}{\pi}\int_0^{\pi/2} \exp\left(-\frac{x^2}{2\sin^2\theta}\right) d\theta$, (10) can be written as

$$\begin{aligned} &P(\mathbf{x}_1 \to \mathbf{x}_2 \mid \hat{\mathbf{p}}) \\ &\quad=\; \frac{1}{\pi}\int_0^{\pi/2} \exp\left(\frac{-|\psi|^2}{4\sin^2\theta(\sigma^2 + \|\mathbf{x}_1\|_2^2\,\sigma_e^2)}\right) d\theta. \end{aligned} \tag{11}$$

Averaging the conditional PEP in (11) over the estimated composite channel vector $\hat{\mathbf{p}}$ through moment generation function (MGF) approach gives

$$\begin{aligned} P(\mathbf{x}_1 \to \mathbf{x}_2) \;&=\; \mathbb{E}_{\hat{\mathbf{p}}}\left[\frac{1}{\pi}\int_0^{\pi/2} \exp\left(\frac{-\eta|\psi|^2}{4\sin^2\theta}\right) d\theta\right] \\ &=\; \frac{1}{\pi}\int_0^{\pi/2} \mathbb{E}_{\hat{\mathbf{p}}}\left[\exp\left(\frac{-\eta|\psi|^2}{4\sin^2\theta}\right)\right] d\theta \\ &=\; \frac{1}{\pi}\int_0^{\pi/2} \mathcal{M}_{|\psi|^2}\left(\frac{-\eta}{4\sin^2\theta}\right) d\theta, \end{aligned} \tag{12}$$

where $\eta = \frac{1}{(\sigma^2 + \|\mathbf{x}_1\|^2\sigma_e^2)}$ and $\mathcal{M}_{|\psi|^2}(.)$ is the MGF of $|\psi|^2$. Defining $\Omega \triangleq (\mathbf{x}_1 - \mathbf{x}_2)(\mathbf{x}_1 - \mathbf{x}_2)^H$, the argument of MGF function, i.e., $|\psi|^2$, can be written in the following form:

$$\begin{aligned} |\hat{\mathbf{p}}(\mathbf{x}_1 - \mathbf{x}_2)|^2 \;&=\; \hat{\mathbf{p}}(\mathbf{x}_1 - \mathbf{x}_2)(\mathbf{x}_1 - \mathbf{x}_2)^H\hat{\mathbf{p}}^H \\ &=\; \hat{\mathbf{p}}\;\Omega\;\hat{\mathbf{p}}^H, \end{aligned} \tag{13}$$

Now, for any Hermitian matrix $\mathbf{Z}$ and a complex vector $\mathbf{a}$, the MGF of $\mathbf{a}^H\mathbf{Z}\mathbf{a}$ is given by [13]

$$\mathcal{M}(s) = \frac{\exp(s\bar{\mathbf{a}}^H\mathbf{Z}(\mathbf{I} - s\mathbf{Q}\mathbf{Z})^{-1}\bar{\mathbf{a}})}{\det(\mathbf{I} - s\mathbf{Q}\mathbf{Z})}, \tag{14}$$

where $\mathbf{Q}$ and $\bar{\mathbf{a}}$ denote the covariance matrix and mean vector of $\mathbf{a}$, respectively, and $\mathbf{I}$ is an identity matrix of proper dimension. Using (14) and (13), the MGF of $|\psi|^2$ can be written as

$$\mathcal{M}_{|\psi|^2}(s) = \frac{\exp(s\bar{\hat{\mathbf{p}}}\mathbf{\Omega}(\mathbf{I} - s\mathbf{Q}\mathbf{\Omega})^{-1}\bar{\hat{\mathbf{p}}}^H)}{\det(\mathbf{I} - s\mathbf{Q}\mathbf{\Omega})}, \tag{15}$$

where $\mathbf{Q}$ and $\bar{\hat{\mathbf{p}}}$ are covariance matrix and mean vector of $\hat{\mathbf{p}}$, respectively, and $\mathbf{I}$ is an identity matrix of order $2^{m_{rf}}$. Using (15) and (12), the average PEP can be written in the following form:

$$\begin{aligned} P(\mathbf{x}_1 \to \mathbf{x}_2) \;&=\; \frac{1}{\pi}\int_0^{\pi/2} \left[\det(\mathbf{I} + \frac{\eta}{4\sin^2\theta}\mathbf{Q}\mathbf{\Omega})\right]^{-1} \\ &\qquad \exp\left[-\frac{\eta}{4\sin^2\theta}\bar{\hat{\mathbf{p}}}\mathbf{\Omega}(\mathbf{I} + \frac{\eta}{4\sin^2\theta}\mathbf{Q}\mathbf{\Omega})^{-1}\bar{\hat{\mathbf{p}}}^H\right] d\theta. \end{aligned} \tag{16}$$

As abstracted by (16), knowledge of only the statistical properties, i.e., mean and covariance of $\hat{\mathbf{p}}$ is required. If kth MAP among the $2^{m_{rf}}$ possible MAPs at the transmitter is activated, then the phase of ith RIS element is

$$\phi_i = -(\angle h_k^i + \angle g^i), \quad i = 1, 2, \cdots, N. \tag{17}$$

So, in the $1 \times 2^{m_{rf}}$ sized composite channel matrix $\hat{\mathbf{p}}$, only the phase of kth channel gain gets nullified. Using central limit theorem (CLT), the statistical properties of different channel gains are given by [3]

$$\mathbb{E}\Big(\sum_{i=1}^{N} h_j^i g^i e^{j\phi_i}\Big) = 0, \quad \mathrm{Var}\Big(\sum_{i=1}^{N} h_j^i g^i e^{j\phi_i}\Big) = N, \tag{18}$$

$\forall j = 1, \cdots, 2^{m_{rf}}$, $j \neq k$. Likewise, for the kth channel gain generated by the used MAP,

$$\mathbb{E}\Big(\sum_{i=1}^{N} |h_k^i||g^i|\Big) = \frac{N\pi}{4}, \quad \mathrm{Var}\Big(\sum_{i=1}^{N} |h_k^i||g^i|\Big) = N\Big(1 - \frac{\pi^2}{16}\Big). \tag{19}$$

The mean vector and covariance matrix of the estimated composite channel vector $\hat{\mathbf{p}}$ can be written as

$$\bar{\hat{\mathbf{p}}} = \mathbb{E}[\hat{\mathbf{p}}] = \Big[0 \quad 0 \cdots \overset{k^{\text{th}}\text{ position}}{\frac{N\pi}{4}} \quad \cdots \quad 0\Big]_{1\times 2^{m_{rf}}}$$

$$\begin{aligned} \mathbf{Q} \;=\; \mathrm{diag}\left(\Big[N \quad N \cdots \overset{k^{\text{th}}\text{ position}}{N\Big(1 - \tfrac{\pi^2}{16}\Big)} \quad \cdots N\Big]_{1\times 2^{m_{rf}}}\right) \\ + \sigma_e^2\mathbf{I}_{2^{m_{rf}}}. \end{aligned} \tag{20}$$

Using (16) and (20), an expression for the bit error rate P_e is given by

$$P_e \leq \frac{1}{2^R}\sum_{\mathbf{x}_1}\sum_{\mathbf{x}_2\neq\mathbf{x}_1}\left\{P(\mathbf{x}_1 \to \mathbf{x}_2)\frac{\delta(\mathbf{x}_1, \mathbf{x}_2)}{R}\right\}, \tag{21}$$

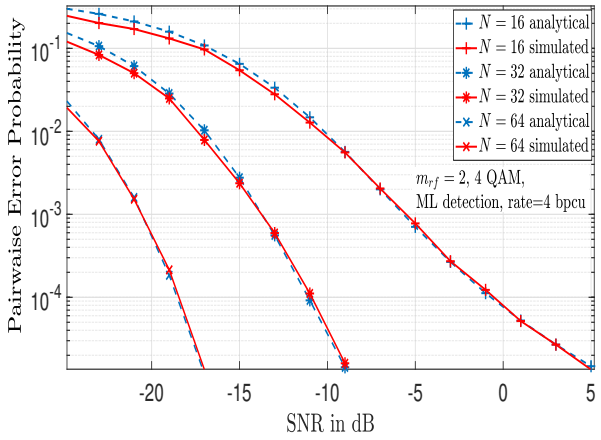

(a) Varying $N = 16, 32, 64$, and $\sigma_e^2 = 0$.

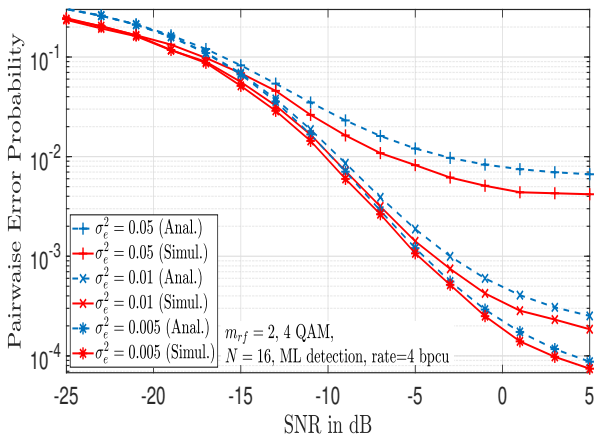

(b) Varying $\sigma_e^2 = 0.005, 0.01, 0.05$, and $N = 16$.

Fig. 2: PEP vs SNR performance of RIS-aided MBM for $\mathbf{x}_1 = [0, 0, -1 + j, 0]^T$ and $\mathbf{x}_2 = [1 - j, 0, 0, 0]^T$.

where $P(\mathbf{x}_1 \rightarrow \mathbf{x}_2)$ is the unconditional PEP, $\delta(\mathbf{x}_1, \mathbf{x}_2)$ represents the difference in the bit patterns of the transmitted signal vectors $\mathbf{x}_1$ and $\mathbf{x}_2$, and $R = m_{rf} + \log_2 M$ is the number of transmitted bits in one channel use.

B. BER analysis with imperfect CSI and phase tuning errors

As mentioned in Sec. II, there can be errors in the phases of the RIS elements due to imperfections in implementation. The phase of the ith RIS element with phase tuning error is given by

$$\phi_i' = -(\angle h_k^i + \angle g^i) - \phi_i^e, \tag{22}$$

and the corresponding phase matrix is given by $\mathbf{\Phi}' = \text{diag}\{e^{j\phi_1'}, \cdots, e^{j\phi_N'}\}$. So, (3) can be rewritten as

$$\begin{aligned} y &= \mathbf{g}\Phi'\mathbf{H}\mathbf{x} + n \\ &= \hat{\mathbf{p}}'\mathbf{x} + n, \end{aligned} \tag{23}$$

where $\mathbf{p}' \triangleq \mathbf{g}\mathbf{\Phi}'\mathbf{H}$ is new composite end-to-end channel matrix which contains phase tuning error. The ML detection is given by

$$\hat{\mathbf{x}} = \min_{\mathbf{x} \in \mathbb{S}} |y - \hat{\mathbf{p}}'\mathbf{x}|^2, \tag{24}$$

where $\hat{\mathbf{p}}' = \mathbf{p}' + \mathbf{e}$ is the estimated channel vector available at the receiver that has both phase tuning and composite channel estimation errors. In order to find the statistical properties of the channel vector, we require $\mathbb{E}(e^{-j\phi_i^e}) = \text{sinc}\left(\frac{1}{L}\right)$ and $\text{Var}(e^{-j\phi_i^e}) = 1 - \text{sinc}^2\left(\frac{1}{L}\right)$.

In the $1 \times 2^{m_{rf}}$ sized channel vector $\mathbf{p}'$, the mean and variance of channel gains that are not corresponding to the used MAP is given by (18). Using CLT, the statistical properties of kth channel gain generated by the used MAP is given by[1]

$$\mathbb{E}\left(\sum_{i=1}^{N} |h_k^i||g^i|e^{-j\phi_i^e}\right) = \frac{NL\sin(\frac{\pi}{L})}{4}$$

$$\text{Var}\left(\sum_{i=1}^{N} |h_k^i||g^i|e^{-j\phi_i^e}\right) = N\left(1 - \frac{\pi^2}{16}\text{sinc}^2\left(\frac{1}{L}\right)\right). \tag{25}$$

The mean vector and covariance matrix of the estimated composite channel vector $\hat{\mathbf{p}}'$ can be written as

$$\bar{\hat{\mathbf{p}}}' = \mathbb{E}[\hat{\mathbf{p}}'] = \begin{bmatrix} 0 & 0 & \cdots & \overset{k^{\text{th}}\text{ position}}{\frac{NL\sin(\frac{\pi}{L})}{4}} & \cdots & 0 \end{bmatrix}_{1 \times 2^{m_{rf}}},$$

$$\mathbf{Q} = \text{diag}\left(\begin{bmatrix} \overset{k^{\text{th}}\text{ position}}{N} & \cdots & N\left(1 - \frac{\pi^2}{16}\text{sinc}^2\left(\frac{1}{L}\right)\right) & \cdots & N \end{bmatrix}_{1 \times 2^{m_{rf}}}\right) + \sigma_e^2 \mathbf{I}_{2^{m_{rf}}}. \tag{26}$$

Using the mean vector and covariance matrix in (26), the BER can be computed using (16) and (21).

IV. Results and Discussions

This section discusses the BER performance of the considered RIS-aided MBM system. In all the simulations, 4-QAM modulation, $m_{rf} = 2$, (i.e., rate of 4 bpcu), and ML detection are used. In Fig. 2, we plot the PEP as a function of SNR for $\mathbf{x}_1 = [0, 0, -1+j, 0]^T$ and $\mathbf{x}_2 = [1-j, 0, 0, 0]^T$. PEP plots obtained through analysis using (16) and simulations are shown. Fig. 2a shows the PEP plots for different number of RIS elements $N = 16, 32, 64$ and $\sigma_e^2 = 0$. It can be seen that the analytical PEP and simulated PEP plots become increasingly close for increasing values of N, showing the effectiveness of the CLT approximation employed in the analysis. Fig. 2b shows the PEP plots for $\sigma_e^2 = 0.005, 0.01, 0.05$ and $N = 16$. As expected, the PEP plots floor at high SNRs because of channel estimation errors, and the floored PEP value increases as σ_e^2 is increased.

In Fig. 3, we show the analytical and simulated BER as a function of SNR for the considered RIS-aided MBM system. Fig. 3a shows the BER plots for varying $N = 16, 128, 256$ and $\sigma_e^2 = 0$. It can be seen that the analytical and simulated BER plots get very close for high SNRs due to the union bounding

[1]If A and B are independent RVs, $\text{Var}\{AB\} = \text{Var}\{A\}\text{Var}\{B\} + \text{Var}\{A\}\mathbb{E}^2\{B\} + \mathbb{E}^2\{A\}\text{Var}\{B\}$ and $\mathbb{E}\{AB\} = \mathbb{E}\{A\}\mathbb{E}\{B\}$.

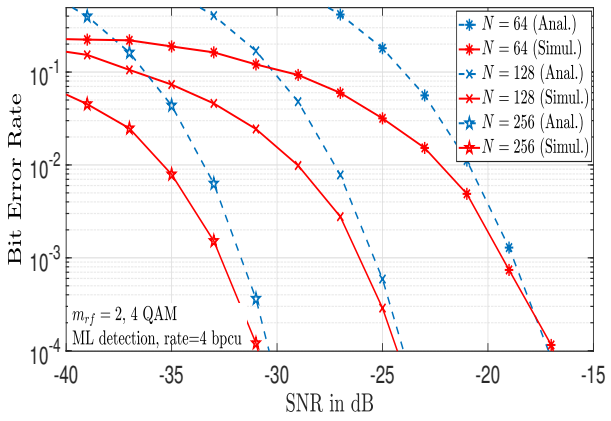

(a) Varying $N = 64, 128, 256$, and $\sigma_e^2 = 0$.

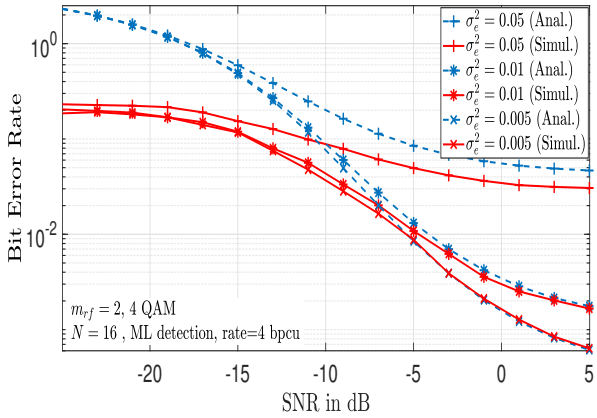

(b) Varying $\sigma_e^2 = 0.005, 0.01, 0.05$, and $N = 16$.

Fig. 3: BER vs SNR performance of RIS-aided MBM in the presence of imperfect CSI at receiver.

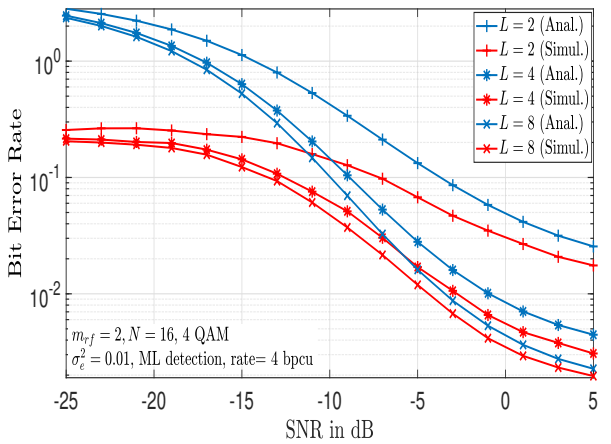

(a) Varying $L = 2, 4, 8$, and $N = 16$, $\sigma_e^2 = 0.01$.

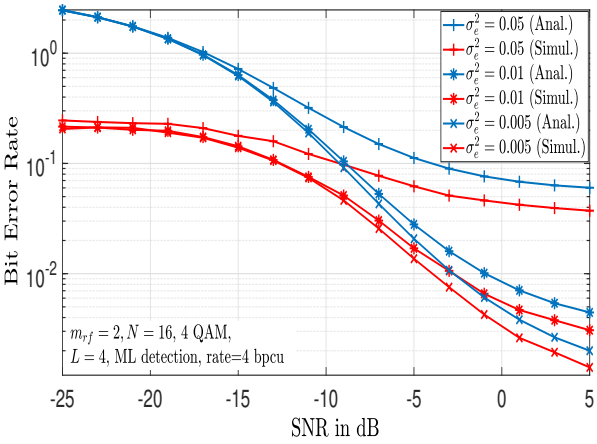

(b) Varying $\sigma_e^2 = 0.005, 0.01, 0.05$, and $N = 16$, $L = 4$.

Fig. 4: BER vs SNR performance of RIS-aided MBM in the presence of imperfect CSI and phase tuning errors.

based expression in (21). Also, as expected, the BER improves as the number of RIS elements N is increased. In Fig. 3b, we see that the BER also floors at high SNRs, and the BER floors at higher BER values for increasing σ_e^2 values. For example, for $\sigma_e^2 = 0.01$, the BER starts flooring at 5 dB SNR at a BER value of about 1.6×10^{-3}, whereas the BER starts flooring at -1 dB SNR at a BER value of about 3×10^{-2} for $\sigma_e^2 = 0.05$.

In Fig. 4, we plot the BER performance of the RIS-aided MBM system affected by both channel estimation and phase tuning errors. In Fig. 4a, analytical and simulated BER curves are plotted for $\sigma_e^2 = 0.01$ with varying $L = 2, 4, 8$. It is seen that the BER degrades with phase tuning errors and this degradation increases with smaller values of L (i.e., increased phase tuning errors). In Fig. 4b analytical and simulated BER curves for $L = 4$ with varying $\sigma_e^2 = 0.005, 0.01, 0.05$ are plotted, which illustrate the degrading effect of increasing σ_e^2 in the presence of phase tuning errors.

V. Conclusions

In this work, we investigated the performance of RIS-aided media-based modulation with imperfect channel state information at the receiver and phase tuning errors at the RIS, which has not been reported before. We derived expressions for the pair wise error probability and bit error probability for this system using moment generating function approach. We presented the BER performance results obtained through analysis and simulations. Our results showed that the performance of RIS-aided MBM improved for increasing number of RIS elements. In future, the BER analysis of RIS-aided MBM system can be explored for multiple-input multiple-output (MIMO) case along with different phase optimization techniques at the RIS.

References

[1] E. Basar, M. D. Renzo, J. de Rosny, M. Debbah, M.-S. Alouini, and R. Zhang, "Wireless communications through reconfigurable intelligent surfaces," *IEEE Access*, vol. 7, pp. 116753-116773, Aug. 2019.

[2] Q. Wu and R. Zhang, "Intelligent reflecting surface enhanced wireless network via joint active and passive beamforming," *IEEE Trans. Wireless Commun.*, vol. 18, no. 11, pp. 5394-5409, Nov. 2019.
[3] E. Basar, "Reconfigurable intelligent surface-based index modulation: a new beyond MIMO paradigm for 6G," *IEEE Trans. Commun.,* vol. 68, no. 5, May 2020.
[4] A. K. Khandani, "Media-based modulation: a new approach to wireless transmission," *Proc. IEEE ISIT'2013*, pp. 3050-3054, Jul. 2013.
[5] Y. Naresh and A. Chockalingam, "On media-based modulation using RF mirrors," *IEEE Trans. Veh. Tech.*, vol. 66, no. 6, pp. 4967-4983, Jun. 2017.
[6] F. Yarkin, I. Altunbas, and E. Basar, "Cooperative space shift keying media-based modulation with hybrid relaying," *IEEE Systems Journal*, vol. 14, no. 1, Mar. 2020.
[7] A. Datta, M. Mandloi, and V. Bhatia, "Minimum error pursuit algorithm for symbol detection in MBM massive-MIMO," *IEEE Commn. Lett.,* vol. 25, no. 2, pp. 627-631, Feb. 2021.
[8] A. Roy, Y. Naresh, A. Padmanabhan, A. Chockalingam, and K. J. Vinoy, "Digitally reconfigurable metasurface array for a multipath based wireless link with media-based modulation," *IEEE Trans. Microwave Theory and Techniques*, vol. 70, no. 12, pp. 5418-5426, Dec. 2022.
[9] Y. Yan, Y. Cao, and T. Lv, "Enabling media-based modulation for reconfigurable intelligent surface communications," *Proc. IEEE WCNC'2021*, pp 1-6, Mar.-Apr. 2021.
[10] Y. Naresh and A. Chockalingam, "Performance analysis of media-based modulation with imperfect channel state information," *IEEE Trans. Veh. Tech.*, vol. 67, no. 5, pp. 4192-4207, May 2018
[11] M. Can, I. Altunbas, and E. Basar, "MBM-aided uplink cooperative NOMA With hardware impairments and imperfect CSI," *IEEE Comm. Lett.*, vol. 25, no. 6, pp. 1830-1834, Jun. 2021.
[12] I. Trigui, E. K. Agbogla, M. Benjillali, W. Ajib, and W. -P. Zhu, "Bit error rate analysis for reconfigurable intelligent surfaces with phase errors," *IEEE Commun. Lett.*, vol. 25, no. 7, pp. 2176-2180, Jul. 2021.
[13] Turin, G. L. "The characteristic function of Hermitian quadratic forms in complex normal variables." Biometrika, vol. 47, no. 1/2, 1960, pp. 199–201. JSTOR, https://doi.org/10.2307/2332977.